

Seasonally varying predation behaviour and climate shifts are predicted to affect predator-prey cycles

Rebecca Tyson

Mathematics and Statistics

IKBSAS 5 BLDG SCI

University of British Columbia Okanagan

1177 Research Road

Kelowna, BC, V1V 1V7

Frithjof Lutscher*

Department of Mathematics and Statistics

Department of Biology

University of Ottawa

585 King Edward Avenue

Ottawa, ON, K1N6N5

June 17, 2018

Keywords: predator-prey model, seasonality, behavioural response, global change

Extended Online Edition: Appendix A,B.

Dryad Link for Code: doi:10.5061/dryad.f2mk6

Manuscript type: Article

Prepared using the suggested L^AT_EX template for *Am. Nat.*

*Both authors contributed equally to this manuscript

Abstract

The functional response of some predator species changes from a pattern characteristic for a generalist to that for a specialist according to seasonally varying prey availability. Current theory does not address the dynamic consequences of this phenomenon. Since season length correlates strongly with altitude and latitude, and is predicted to change under future climate scenarios, including this phenomenon in theoretical models seems essential for correct prediction of future ecosystem dynamics. We develop and analyze a two-season model for the great horned owl (*Bubo virginialis*) and snowshoe hare (*Lepus americanus*). These species form a predator-prey system in which the generalist to specialist shift in predation pattern has been documented empirically. We study the qualitative behaviour of this predator-prey model community as summer season length changes. We find that relatively small changes in summer season length can have a profound impact on the system. In particular, when the predator has sufficient alternative resources available during the summer season, it can drive the prey to extinction; there can be coexisting stable states; and there can be stable large-amplitude limit cycles coexisting with a stable steady state. Our results illustrate that the impacts of global change on local ecosystems can be driven by internal system dynamics and can potentially have catastrophic consequences.

Introduction

Traditional predator-prey theory classifies predators as being either “specialist” or “generalist”, but what if the actual predator-prey relationship varies seasonally? In the traditional view, predation behaviour is an inherent property of the interaction between two particular species. Accordingly, predator-prey theory is based on dynamic models that use different functional responses to distinguish specialist from generalist predators, and these functional forms are fixed over time. Seasonal variations in food supply however, can have a strong effect on the functional response within a given predator-prey relationship (van Leeuwen et al., 2007), so that a predator appears to respond to prey density as a generalist when many prey species are available, but as a specialist when few species are present (see examples below).

We use the term “behaviour shift” to describe the qualitative seasonal change in functional response from a concave shape (Holling Type II), typically associated with a specialist predator, to a sigmoid shape (Holling type III), representing generalist predation. There is currently no theory in place to address the dynamic consequences of this shift in behaviour. Theoretical models have addressed other aspects of seasonal variation, for example, the effects of seasonally varying strength of interaction in predator-prey communities (Taylor et al., 2013; Turchin and Hanski, 1997) and in disease transmission dynamics (Bacaër, 2012; Keeling and Rohani, 2008). Seasonality is included in these models by having key parameters take on season-specific values, resulting in quantitative changes in certain processes, such as contact rates or growth rates. These studies and have shown that seasonality modeled in this way is a key factor in system dynamics.

We are interested in a more fundamental, qualitative shift of the interaction through the seasons, not only a quantitative change. We anticipate that such a behavioural shift could have significantly more dramatic effects on predator-prey dynamics. The interaction of specialist predators with their prey can drive population cycles through strong, delayed negative feedback loops (Berryman, 1989). Generalist predators, on the other hand, are thought to produce weaker feedback (Maynard Smith, 1974) and thus have a damping effect on cycles (Bjørnstad et al., 2010; Turchin and Hanski, 1997). The combination of these effects through seasonal “behaviour shift” could potentially result in fundamentally new system dynamics.

Understanding the effects of seasonal variation on ecosystems is particularly relevant in the context of global change, which is inexorably altering seasonal patterns. Changes in season length can potentially disrupt predator-prey system dynamics and put organisms at risk of extinction, if key aspects of the interaction vary seasonally. Indeed, predicting species persistence and population dynamics under changing climates is a pressing challenge (Leroux et al., 2013; Molnàr et al., 2010). How then does global change affect predator-prey systems when there is

a seasonal behavioural shift in predation? Motivated by experimental data on great horned owl (*Bubo virginialis*) behaviour from the boreal forest (a region particularly vulnerable to climate change (Allen et al., 2013; IPCC Working Group I, 2007)), we use a novel, time-periodic predator-prey model to address this question.

A generalist to specialist behaviour shift was identified in the great horned owl in the boreal forest. The long-term monitoring project in the Kluane, Yukon Territory, Canada, provides data on gut content of the great horned owl, indicating that its predation pattern changes from specialist in the winter to generalist in the summer (Rohner et al. (2001), Figure 15.6). In winter, snowshoe hares (*Lepus americanus*) represent a consistently high percentage (typically over 80%, except in 1994) of the diet, with usually only one other prey species consumed. In addition, experimental data on snowshoe hare predation by great horned owls exhibit a type II functional response, confirming that the great horned owl is a specialist during the winter. In summer, snowshoe hare is still prominent in the owl diet, but its percentage varies greatly and closely reflects the changes in available hare density. There are typically at least four other prey species present. Data on summer predation by owls is best fit with a type III functional response typical of a generalist predator (Rohner et al. (2001), Figure 15.9). Thus, the relationship between the great horned owl and the snowshoe hare exhibits a seasonal behaviour shift from specialist-type predation in the winter to generalist-type predation in the summer.

This strong seasonal shift is not limited to the owl-hare system. Evidence for behaviour shifts in functional response also exists in Alaska where the bald eagle (*Haliaeetus leucocephalus*) preys on Canada geese (*Branta canadensis*) (Miller et al., 2006). In Nova Scotia, the coyote (*Canis latrans*) preying on white-tailed deer (*Odocoileus virginianus*) and snowshoe hares also exhibits a seasonal behaviour shift (Patterson et al., 1998).

Historically, models for predator-prey interactions study dynamical behaviour in the context of one functional response (e.g. Strohm and Tyson (2009)) or compare the effects of different functional responses (e.g. Freedman and Wolkowicz (1986)). Universally, however, the functional response is considered a fixed characteristic of the predator. If seasonal variation is included, the standard approach is to vary individual model parameters while preserving the basic shape (generalist or specialist) of the functional response. Such approaches consider quantitative seasonal variation in the strength of predation, and can explain latitudinal variation in population cycles of voles (Taylor et al., 2013; Turchin and Hanski, 1997). These models also generate challenges for mathematical analysis (Gragnani and Rinaldi, 1995; Rinaldi et al., 1993). None of these models, however, can capture a fundamental qualitative change in the process itself, such as the behaviour shift in predation described above.

We present and analyze a two-season model for one focal prey and one predator, wherein the predator is a specialist in the winter and a generalist with alternative food sources during the summer. We study in detail how the dynamics of this system change when season length varies. An increase in summer season can represent

decreasing latitude or altitude and/or future climates under global change. We find that the model dynamics are relatively simple when the alternative resources in the summer are insufficient to sustain the predator in the absence of the focal prey. When alternative resources are abundant, the system can generate unexpected dynamics such as prey extinction or large-amplitude limit cycles. We show that the response of communities to climate change goes beyond the simple question of species persistence or extirpation and includes abrupt qualitative changes in community dynamics.

Model and methods

Formulating a predator-prey model for discrete seasons

For a minimal model that captures the processes described above, we consider a predator-prey system in a two-season environment, where the summer season lasts for a fraction, $0 \leq T_s \leq 1$, of the year. During the summer, the focal prey (N) grows logistically and is subject to predation by a generalist predator (P) with a type III (Holling, 1959) functional response (Rohner et al. (2001), Figure 15.9). The generalist predator grows in a logistic-like fashion, independent of the focal prey, and enhances its growth rate by consuming the focal prey when sufficiently abundant. The equations describing summer dynamics read (Erbach et al., 2013)

$$\frac{dN}{dt} = rN \left(1 - \frac{N}{K} \right) - \frac{aN^2P}{b^2 + N^2}, \quad \frac{dP}{dt} = \gamma \frac{aN^2P}{b^2 + N^2} + \frac{sP}{1 + \nu P} - mP. \quad (1)$$

For a description of parameters, see Table B.1. A similar model with a type II functional response was studied by Magal et al. (2008). In the standard model for prey and generalist-predator dynamics, the predator has insufficient or no alternative resources. It cannot sustain itself in the absence of the focal prey (Morozov and Petrovskii, 2009) (see Erbach et al. (2013) for a criticism and detailed discussion of this assumption). This standard scenario arises in our model when $\nu = 0$ and $s - m < 0$.

During the winter season, predation continues to be the preeminent cause of prey death (Rohner et al., 2001), whereas prey growth is negligible due to scarcity of resources. Because alternative prey are unavailable, the predator acts as a specialist with type II functional response (Rohner et al. (2001), Figure 15.9). Hence, the model for the winter dynamics differs from the summer model not simply through parameter values but through a qualitatively different functional response characterising the process of predation. Predator growth occurs only from predation on the focal prey according to a type II numerical response. We choose the equations

$$\frac{dN}{dt} = -\frac{\alpha NP}{\beta + N}, \quad \frac{dP}{dt} = \gamma \frac{\alpha NP}{\beta + N} - \mu P. \quad (2)$$

The parameters in equation (2) are explained in Table B.1.

To formulate our complete seasonal model, we alternate equations (1) and (2) according to season. Our basic time unit is one year, and we choose time $t = 0$ to mark the beginning of summer. Then equations (1) are valid for $0 \leq t < T_s$, while equations (2) are valid for $T_s \leq t < 1$, and are periodically alternating from then on. In particular, the switch between seasons is instantaneous. Population densities remain continuous, that is, the densities at the end of one season serve as initial densities for the next season. To simplify the analysis and identify the important parameter combinations, we scale the hare populations by their carrying capacity K , and the predator population by the quantity rK/a , which is the hare population growth rate divided by the maximum per predator kill rate. With this scaling, we can write the model using dimensionless densities $n = N/K$, and $p = aP/(rK)$ and time $\tau = tr$. Our complete seasonal model then reads

$$\begin{aligned} \text{summer :} \quad & \frac{dn}{d\tau} = n(1-n) - \frac{n^2 p}{\tilde{b}^2 + n^2}, & \frac{dp}{d\tau} &= \tilde{\gamma} \frac{n^2 p}{\tilde{b}^2 + n^2} + \tilde{s} \frac{p}{1 + \tilde{v} p} - \tilde{m} p \\ \text{winter :} \quad & \frac{dn}{d\tau} = -\frac{\tilde{\alpha} n p}{\tilde{\beta} + n}, & \frac{dp}{d\tau} &= \tilde{\gamma} \frac{\tilde{\alpha} n p}{\tilde{\beta} + n} - \tilde{\mu} p, \end{aligned} \quad (3)$$

where $\tilde{\alpha} = \alpha/a$, $\tilde{\beta} = \beta/K$, $\tilde{b} = b/K$, $\tilde{m} = m/r$, $\tilde{\mu} = \mu/r$, $\tilde{s} = s/r$, $\tilde{v} = vrK/a$ and $\tilde{\gamma} = \gamma a/r$.

We obtain parameter estimates for the interaction between the great horned owl and snowshoe hare from the literature (Table B.1). According to these values, the ranges for scaled parameters are $\tilde{\alpha} = 0.40 - 2.7$, $\tilde{\beta} = 0.004 - 0.6$, $\tilde{b} = 0.07 - 0.3$, $\tilde{m} = \tilde{\mu} = 0.07 - 0.4$, $\tilde{s} = 0.07 - 0.9$, $\tilde{\gamma} = 0.33 - 1.0$. From this point forward, we drop tildes to simplify notation.

Preliminary Observations and Analytic Approach

To understand the dynamics of the seasonal model we need to understand the dynamics of its parts. The dynamics of the winter model (2) alone are simple: Prey density decreases, predator density may initially increase, but eventually both approach zero. The dynamics of the summer model (1) are considerably more complex. When the predator has insufficient alternative resources ($v = 0$, $s - m < 0$), predator and prey stably coexist when $b > K/\sqrt{27}$ (or $\tilde{b} > 1/\sqrt{27} \approx 0.19$), but when $b < K/\sqrt{27}$ stable limit cycles are possible (Morozov and Petrovskii, 2009). With sufficient alternative resources ($s > 0$), a detailed bifurcation analysis found four key

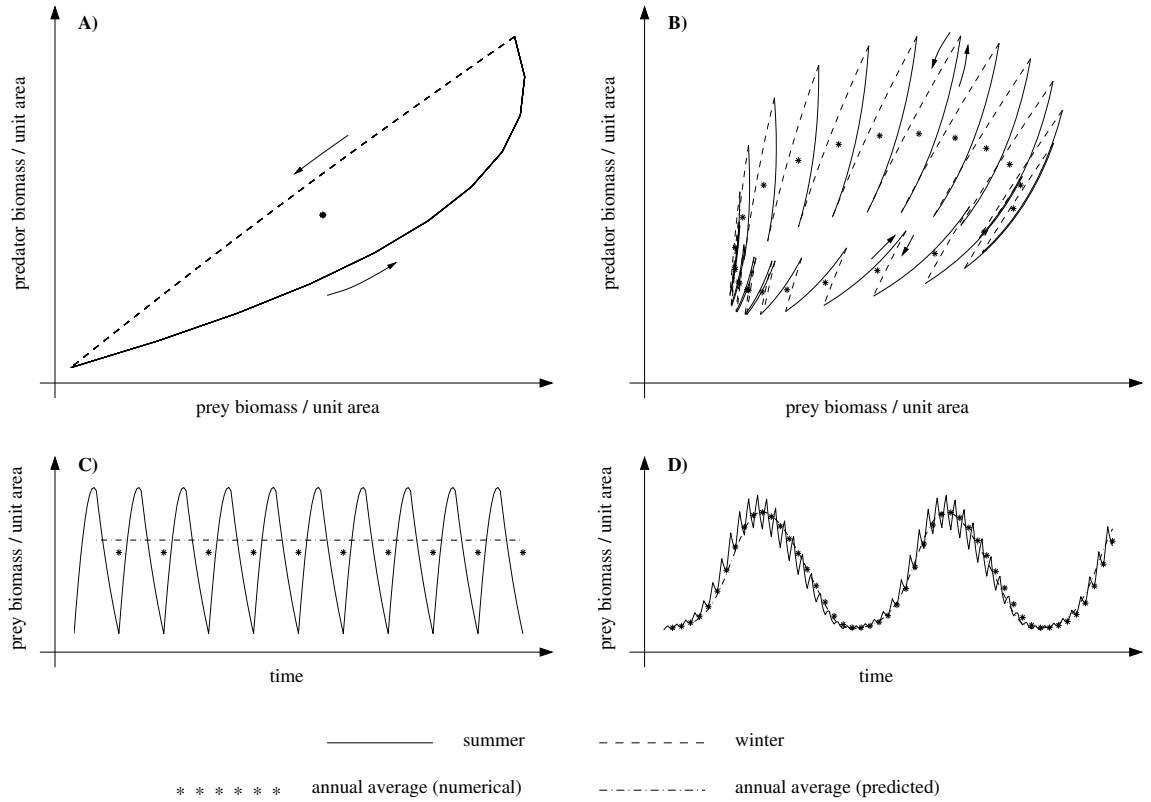


Figure 1: Two typical long-term scenarios in the two-season model (3): Annual variation (panels A and C) and multi-annual cycles (panels B and D). In the phase-plane plots (panels A and B), arrows indicate the direction of solutions during the summer (solid lines) and winter (dashed lines). Corresponding time series plots (panels C and D) show prey density of the annual model (solid lines) and the averaged model (dash-dotted lines). Asterisks indicate annual averages of the seasonal model.

scenarios (Erbach et al., 2013): Depending on parameter values, prey and predator can (1) stably coexist or (2) cycle, there can be (3) two alternative stable coexistence states or (4) a stable coexistence state surrounded by a stable limit cycle. Similar dynamics arise with a type II functional response (Magal et al., 2008).

Seasonal model (3) with annual variation has only two steady states: the zero state when predator and prey are both absent, and the prey-only state, when the predator density is zero. The stability conditions for these states can be calculated explicitly (Online Appendix A), but are not our focus here. All other solutions exhibit (at least) annual variation: Prey density decreases in the winter but may increase in the summer, whereas predator density may increase or decrease in either season. We illustrate the two main, qualitatively different long-term scenarios of the seasonal model in Figure 1. In the first scenario (panels A and C), we observe only annual variation where both densities decrease during the winter and increase during the summer. The increase exactly offsets the decrease; the yearly average remains constant. In the second scenario (panels B and D), the yearly average exhibits a multi-annual, quasi-periodic cycle, and within each year densities of prey and predator fluctuate.

Aside from numerical simulations, there are no explicit techniques available to study our two-season model.

Instead, we use temporal averaging to derive a much simpler predator-prey model that still contains the basic mechanisms that we study here. Temporal averaging applies to systems with inherently different time scales. Mathematical theory shows that the dynamics of such systems are mostly determined by the slow time scale behaviour, appropriately averaged over the fast time scale (Guggenheimer and Holmes, 1983). In our case, population dynamics represent the slow time scale whereas seasonal variation occurs on a fast time scale. Accordingly, the temporally averaged equations for model (3) consist of the weighted sum of the right-hand sides of (3) with weights according to the relative season lengths. The averaged model is *not* an exact model for the averages of the seasonal model, but only an approximation. To distinguish between the seasonal and the averaged model, we denote prey and predator densities in the averaged model as x and y , respectively. The model reads

$$\begin{aligned}\frac{dx}{d\tau} &= T_s \left[x(1-x) - \frac{x^2 y}{b^2 + x^2} \right] + (1 - T_s) \left[-\frac{\alpha xy}{\beta + x} \right] \\ \frac{dy}{d\tau} &= T_s \left[\gamma \frac{x^2 y}{b^2 + x^2} + s \frac{y}{1 + \nu y} - my \right] + (1 - T_s) \left[\gamma \frac{\alpha xy}{\beta + x} - \mu y \right].\end{aligned}\tag{4}$$

This averaged model can be analyzed with standard phase-plane techniques (see below). Plotting the solutions of (4) (Figure 1, panels C and D, dashed lines) indicates that the averaged model can approximate the averages of the two season model fairly well. The averaged model slightly over-predicts averaged densities in the first scenario but is virtually indistinguishable from averaged densities in the scenario of multi-annual cycles. In the following, we will present results from extensive numerical simulations of the two-season model (3) and use the averaged model (4) to gain deeper insights into these dynamics.

Results

We focus our analysis on the effect that a change of season length has on the dynamics. An increase in summer season length can represent decreasing latitude or altitude, or can represent future climates under global change. For simplicity and comparison purposes, we begin with the standard model of insufficient alternative resources for the generalist predator. All numerical solutions were produced in Matlab (Tyson, 2016).

Predator with insufficient alternative resources

When the predator has insufficient alternative resources ($\nu = 0$, $s - m < 0$), it cannot persist in the absence of the focal prey in the standard model, i.e. equations (1), and the same is true for the two-season model. In the presence

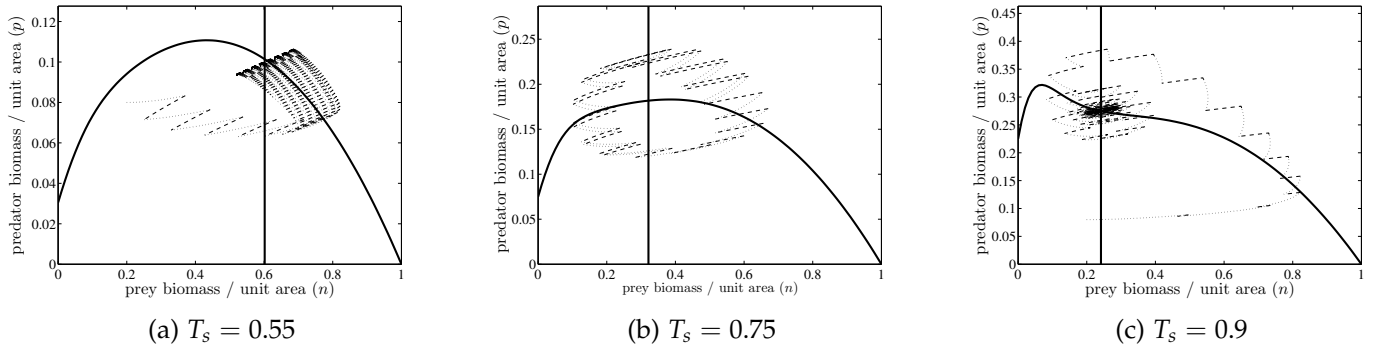


Figure 2: Solution trajectories of the seasonal model (3) in the phase plane for three different values of T_s . Solution trajectories in Panels A and C include transient and steady state behaviour; the solution trajectory in Panel B shows only the long-term behaviour. The steady-state behaviour in each case is: (A) Annual variation for $T_s = 0.55$. (B) Multi-annual cycles for $T_s = 0.75$. (C) Annual variation for $T_s = 0.9$. Solid lines correspond to nullclines of the averaged model (4). Parameters are $b = 0.25$, $\alpha = 2$, $\beta = 0.05$, $s = 0.5$, $m = \mu = 0.6$. and $\gamma = 0.25$.

of the focal prey the predator can persist under certain conditions. Roughly speaking, the total predator growth rate over a year is large enough for persistence if prey density is high enough, predation is frequent enough and predator death is small enough, see Online Appendix A for details. For parameter values within the range of the great-horned owl and snowshoe hare system, coexistence of the two species is guaranteed for large enough values of T_s . Numerical simulations show the two long-term behaviours described in Figure 1: annual variation with constant average or multi-annual cycles. As the season length changes, the dynamics of the system may switch from one to the other (see Figure 2).

When the summer season is short, prey growth is insufficient to sustain a predator population (plot not shown); but as the summer season lengthens, the predator persists in the system. For example, for $T_s = 0.55$ the two species coexist with seasonal variation and constant annual averages (Figure 2, panel A). The annual average of the prey population decreases with increasing summer season length, while the corresponding predator density increases. Both populations should benefit from a longer summer season, but the predator benefits more. As T_s increases further, we eventually observe sustained multi-annual oscillations (e.g. $T_s = 0.75$, Figure 2, panel B). For even longer summers, the multi-annual cycles disappear and the prey density stabilises at a low yearly average (e.g. $T_s = 0.9$, Figure 2, panel C). The corresponding predator density is high. The annual averages of prey and predator show damped oscillations. These changes in the dynamics are summarized in Figure 3, panel A. We simulated the seasonal model until transients had died out and then recorded the maximum and minimum yearly average for the subsequent 50 years. For short and long summers, the average maximum and minimum densities are the same: annual averages remain constant, variation is limited to within years. For intermediate summer length, the annual averages show large limit cycles.

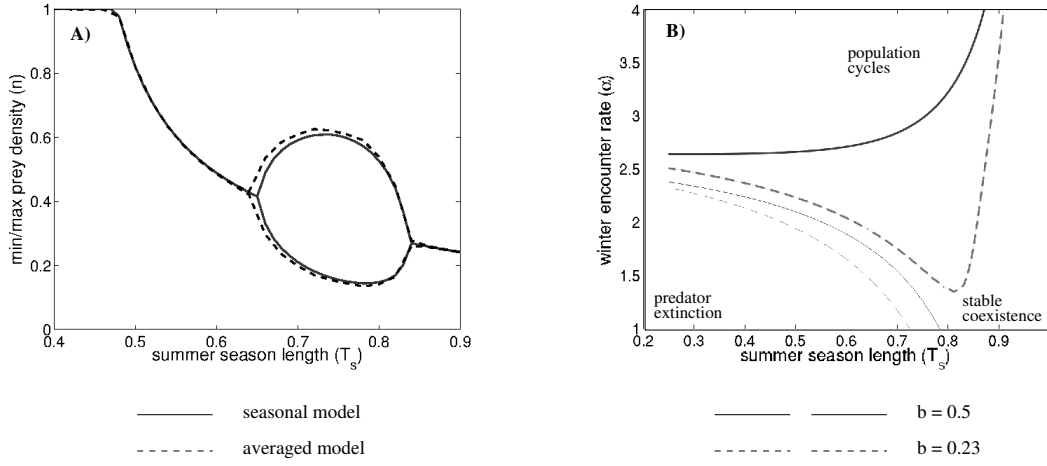


Figure 3: Panel A: Prey density as a function of summer season length: average of the seasonal model (solid) and averaged model (dashed). Maximal and minimal values are plotted after transients have disappeared. Panel B: Stability as a function of T_s and α for small (dashed) and large (solid) values of b (solid lines: $b = 0.5$, dashed lines: $b = 0.23$). For each pair of lines (solid or dashed) there is a thin line and a thick line. Below the thin line, the predator cannot persist in the system according to (7). Between the thin and thick lines, predator and prey stably coexist. Above the thick lines, the populations cycle. All other parameters are as in Figure 2.

Two mechanisms contribute to the transition from predator extinction to stable coexistence as summer season length increases. The effective annual growth rate of the prey increases so that prey biomass approaches carrying capacity faster. Summer season also has the higher predator growth rate. So, as season length increases, predator biomass grows more during the summer, and since prey biomass is greater at the end of the summer, growth will continue somewhat into the winter, so that the predator can eventually persist when T_s is large enough. As T_s increases more, the negative feedback loop becomes so strong that stable coexistence gives way to cycles, as is known from the Rosenzweig-MacArthur model. The eventual disappearance of cycles and stabilization of the coexistence state for large T_s does not arise in the Rosenzweig-MacArthur model but is due to the generalist functional response in our model. The prey density falls to such low levels that the type III functional response is not strong enough to enforce the required negative feedback. The populations stabilise.

To understand these dynamics better, we study the corresponding averaged model (4) via standard phase-plane techniques. The prey nullcline is given by the equation

$$P(x) = \frac{T_s(1-x)}{\frac{T_s x}{b^2+x^2} + \frac{(1-T_s)\alpha}{\beta+x}}, \quad (5)$$

whereas the predator nullcline is a vertical line at $x = x^*$, given by the equation

$$T_s \left[\frac{\gamma(x^*)^2}{b^2 + (x^*)^2} + (s-m) \right] = (1-T_s) \left[\frac{\gamma\alpha x^*}{\beta + x^*} - \mu \right]. \quad (6)$$

Both nullclines are included in the plots in Figure 2. There is a meaningful coexistence state only when $0 < x^* < 1$ or, equivalently, when α is large enough, i.e. when

$$\alpha > \frac{T_s(\frac{\gamma}{b^2+1} + s - m) - (1 - T_s)\mu}{(T_s - 1)\frac{\gamma}{\beta+1}}. \quad (7)$$

Since the predator nullcline is vertical, the coexistence state is stable exactly when the slope of the prey nullcline at this state is negative. For the three cases in Figure 2, the averaged model has a stable coexistence point for $T_s = 0.55$ and $T_s = 0.9$, and a stable limit cycle for $T_s = 0.75$. This prediction clearly agrees with the simulations of the seasonal model.

Moreover, the averaged model also predicts the amplitude (and period) of the yearly averages of the seasonal model in the case of multi-annual cycles (Figure 3, panel A). Dashed lines indicate the maximum and minimum prey density of the averaged model over a 50-year period after transients have disappeared. Due to this surprisingly good agreement between the average of the seasonal model and the averaged model, we can use the simpler averaged model to explore how season length affects population dynamics. Panel B in Figure 3 illustrates how the transition between a stable coexistence point and limit cycles (a Hopf bifurcation in the averaged model) depends on winter killing rate (α) and summer half-saturation constant (b). When summer predation saturates slowly ($b = 0.5$), the Hopf bifurcation line is monotone increasing: as the summer season becomes longer, stronger winter predation is necessary to generate the required negative feedback that drives population cycles. This relationship indicates that cycles are driven by specialist predation in the winter. On the other hand, when summer predation saturates quickly ($b = 0.23$), the Hopf bifurcation line is decreasing for a wide range of T_s and only increases as T_s approaches 1. In this case, summer predation is higher at lower values of b and thereby acts to strengthen the negative feedback loop. This effect becomes stronger as summer season length increases and only disappears for very long summers (due to the type III functional response).

Predator with sufficient alternative resources

In the previous scenario, the generalist predator could not survive in the absence of the focal prey. A true generalist can survive on a range of different prey types and is not overly dependent on one particular prey. Thus, we consider the case $\nu > 0$ and $s > m$. However, with this choice, the model for the summer season alone shows a complex bifurcation structure (Erbach et al., 2013). Since a complete analysis of the corresponding seasonal model is beyond the scope of this work, we focus on explaining two novel scenarios and their implications in detail.

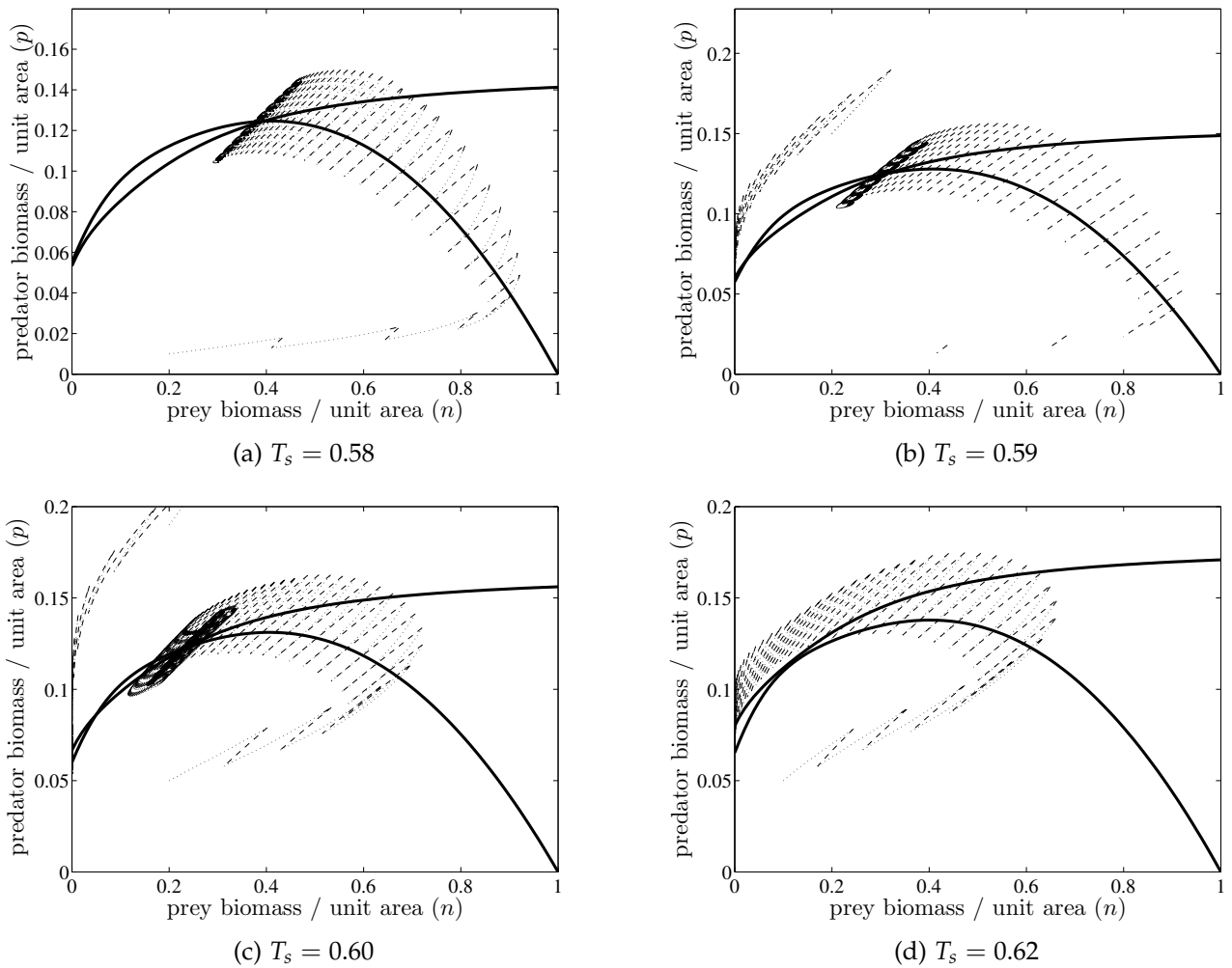


Figure 4: Simulation of the seasonal model (3) when the generalist predator has sufficient alternative resources to survive in the absence of prey. Solution trajectories shown include transient and steady-state behaviour. Panel A: The coexistence state with only annual variation is globally stable when $T_s = 0.58$. Panels B and C: The coexistence state and the prey extinction state are both locally stable when $T_s = 0.59$ and $T_s = 0.6$. In the latter case, the annual averages approach the coexistence state with damped oscillations. Solution trajectories for two different initial conditions are shown. Panel D: The prey extinction state is globally stable when summers are long, $T_s = 0.62$. Parameter values are: $\gamma = 0.07, b = 0.25, s = 1, v = 3, m = \mu = 0.5, \alpha = 2, \beta = 0.08$.

Scenario 1: Extinction of the Prey

When the predator has a positive growth rate in the summer, independent of focal prey density ($v > 0$ and $s > m$), then it can persist in the system when the summer season is long enough (Online Appendix A). Simulations of the seasonal model demonstrate that it may even drive the prey to extinction when the summer season is particularly long (Figure 4).

When the summer season is relatively short, but long enough for the predator to persist, then it will coexist with its prey at constant average density with annual variation (Figure 4, panel A). All solutions approach this state. When the summer season is very long, the prey is driven to extinction; only the predator survives (Figure 4,

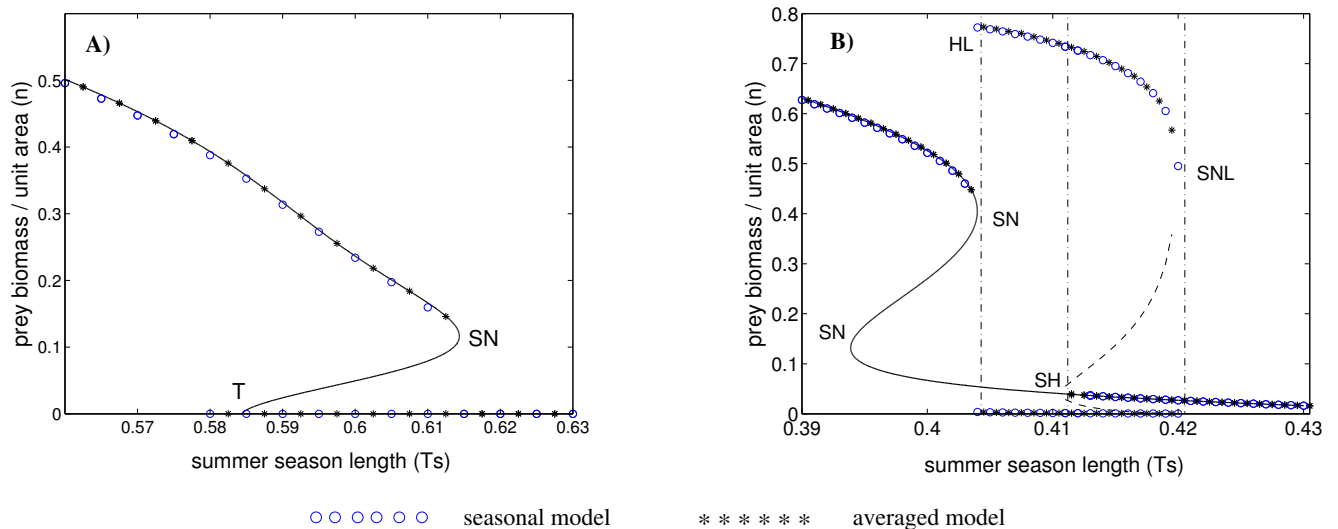


Figure 5: Qualitative behaviour of the seasonal (3) and averaged (4) model as a function of summer season length. Panel A: Prey extinction scenario. Panel B: Large limit cycle scenario. Thin solid lines indicate the prey steady-state value in the averaged model. Thin dashed lines represent the maximum and minimum of an unstable limit cycle. Asterisks correspond to simulation results (maxima and minima after the disappearance of initial transients) of the averaged model (4) with two different initial conditions (one in the basin of attraction of the upper steady state, and one outside of this basin and leading to prey extinction). Open circles indicate the corresponding simulations of the seasonal model (3). SN denotes a saddle-node bifurcation in the averaged model, T a transcritical bifurcation. SH stands for subcritical Hopf bifurcation, HL and SNL indicate a homoclinic loop bifurcation and a saddle-node bifurcation of limit cycles (see explanation in the text). The vertical dash-dot lines only serve to provide visual structure to the reader. In panel B, the homoclinic loop bifurcation occurs just before the saddle-node bifurcation. Parameter values are $\gamma = 0.07, b = 0.25, s = 1, v = 3, m = \mu = 0.5, \alpha = 2$, and $\beta = 0.08$ for panel A and $\gamma = 0.05, b = 0.05, s = 1, v = 3, m = \mu = 0.4, \alpha = 2$, and $\beta = 0.1$ for panel B.

panel D). All solutions approach the axis where prey density is zero but retain positive predator density. Its alternative resources during the summer months allow the predator to maintain high population densities. The type II functional response in the winter results in high (per capita) predation pressure even at low focal prey density. In the transition between these two extremes we observe coexistence of two locally stable states. Panels B and C in Figure 4 each depict two solutions, one that approaches the prey-extinction state and one that approaches a coexistence state with annual variation. In Panel C, the annual averages approach the positive steady state with damped oscillations. No such oscillations are present in panel B. These qualitative changes are summarized in Figure 5, where we plot the average annual prey-density at stable steady-states (open circles, panel A). Exact but implicit conditions for prey growth at low densities are given in Online Appendix A.

Coexisting stable states (or bistability) often arise when a pair of steady states emerge as a parameter changes. A famous example is the spruce budworm model (Ludwig et al., 1978). As the two steady states are a saddle and a node, this bifurcation is called a saddle-node or fold bifurcation. Our analysis of the corresponding averaged model (4) reveals precisely this expected structure (Figure 4). The model nullclines intersect twice when $T_s \leq 0.6$. The

intersection corresponding to larger prey density is a stable node, the intermediate one a saddle. As T_s increases, the two steady states collide and disappear in a saddle-node bifurcation. For larger T_s , all solutions converge to the prey-extinction state. The solid curve in Figure 5, panel A, represents the prey density at the positive steady states; it has two branches in the interval $0.585 < T_s < 0.615$. The asterisks in the figure represent stable steady states arising from numerical simulations of the averaged model (4) with different initial conditions, one in the basin of attraction of the coexistence steady state, and one outside this basin culminating in prey extinction. The open circles are the annual average of simulations of the seasonal model (3) using the same two initial conditions. As in the previous case, the averaged model predicts the qualitative and quantitative behaviour of the annual average of the seasonal model very well. The only feature of the seasonal model that the averaged model cannot capture is the oscillatory approach to the coexistence state for $T_s = 0.6$ (Figure 4, panel C). Oscillations are impossible near the coexistence state in the averaged model. Annual variation allows solutions to “jump” across the nullclines, thus generating these oscillations.

Three mechanisms interact to produce this bistability scenario: (i) the predator can sustain itself on alternative prey in the summer; (ii) the predator is a specialist in the winter; (iii) the type III functional response in the summer leads to a low per-capita predation pressure (i.e. $aNP/(b^2 + N^2)$) at low and high prey density. The highest per-capita predation pressure occurs at intermediate prey density. An increase in summer season length boosts predator density in the absence of the focal prey. During the summer, the focal prey population could grow from low density because generalist predation pressure is negligible. During the winter, however, a high predator density exerts strong predation pressure even at low focal prey density, because of the specialist functional response. For this reason, the prey population is unable to grow from low density when summer seasons are long enough ($T_s \approx 0.585$ in Figure 5, panel A). The prey extinction state is stable.

At high prey density, summer predation boosts predator density and is a significant source of prey mortality, but the effect is limited by the maximum predation rate. If the prey density at the end of the summer is still sufficiently high and the predator density sufficiently low then the prey can survive the winter in reasonably high numbers and thrive again in the subsequent summer. Hence, an initially high enough prey density can persist in the system if summers are short enough ($T_s \approx 0.615$ in Figure 5, panel A). The coexistence state is stable.

If the prey-extinction state becomes stable before the coexistence state is destroyed, we observe two coexisting stable states ($0.585 < T_s < 0.615$ in Figure 5, panel A). At intermediate prey density, per-capita predation is maximized in the summer so that predator density at the end of the summer is relatively high and prey density is relatively low. As a result, the prey succumbs to the high predation pressure during the winter and cannot recover the following summer. If the predator behaved as a generalist during the winter season as well, prey extinction

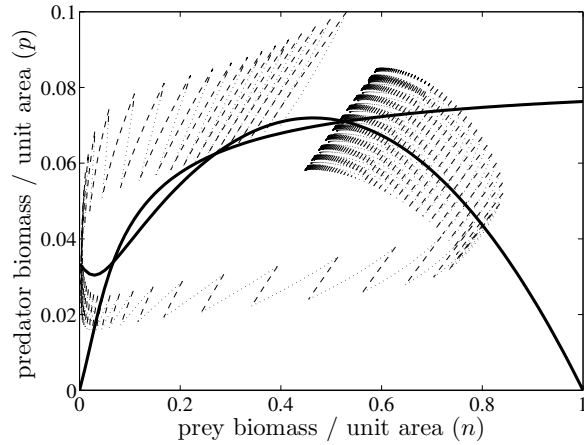
could not occur.

Scenario 2: Large limit cycles

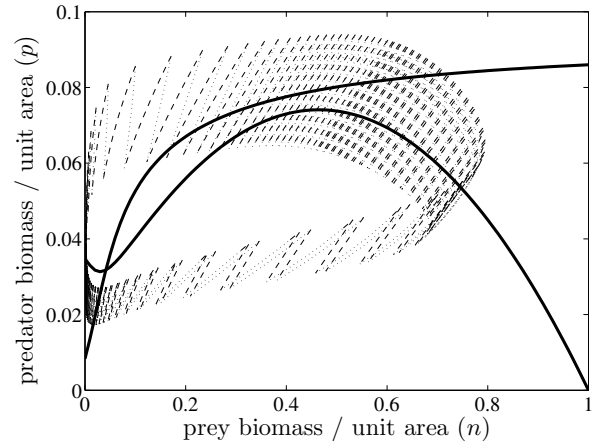
In this second scenario, we significantly reduce the half-saturation constant for summer predation, b , as compared to the previous section, but keep similar values for all other parameters. As a result, we observe a complex combination of the bistable structure observed in the previous section combined with a limit cycle (Figure 6). When summers are short, the two populations coexist with constant annual average at high densities (panel A). Increasing summer length destabilises the system so that multi-annual oscillations with large amplitudes of the annual averages arise (Figure 6, panel B). While these oscillations persist, a coexistence state with constant annual averages at low density becomes stable (Figure 6, panel C). For even longer summers, the multi-annual cycles disappear, and all solutions approach the coexistence state with low-density annual averages (Figure 6, panel D). A summary of these transitions is depicted in Figure 5, panel B. For much longer summers, the prey goes extinct and the predator persists as in the previous scenario (plot not shown).

The corresponding averaged model is, again, a very good predictor of the average of the seasonal model, and helps explain the various transitions that we observe (Figure 5, panel B). When T_s is small, predator and prey coexist stably at high prey density. As T_s increases, two steady states emerge (saddle-node bifurcation), but both are unstable ($T_s \approx 0.394$). Just before the stable coexistence point and the intermediate saddle collide and disappear (again a saddle-node bifurcation), a large limit cycle appears ($T_s \approx 0.404$). Mathematically, this limit cycle does not arise from a steady state through a Hopf bifurcation as we saw earlier, but through a so-called homoclinic loop bifurcation (see Erbach et al. (2013) for a detailed explanation of a similar situation). The unstable coexistence state becomes stable ($T_s \approx 0.41$), where an unstable limit cycle emerges. Mathematically speaking, this is a Hopf bifurcation, but in contrast to the previous case, it is subcritical now, meaning that the emerging limit cycle is unstable. The stable and unstable limit cycles collide and annihilate one another ($T_s \approx 0.42$). Only the stable coexistence state at low prey density remains. This annihilation of limit cycles is similar to the annihilation of two steady states in a saddle node bifurcation, and is therefore called a saddle-node bifurcation of limit cycles ($T_s \approx 0.42$).

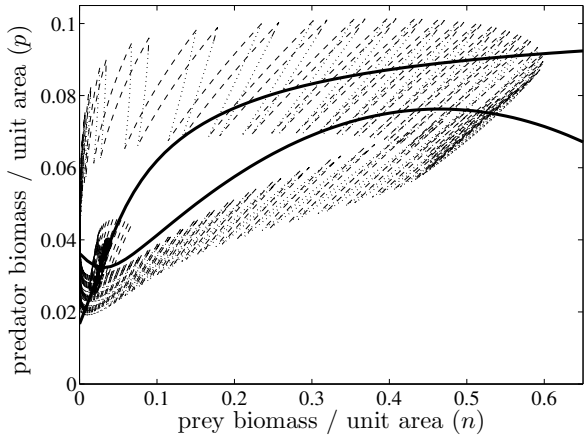
The averaged model predicts the dynamic behaviour of the seasonal model, including cycle amplitude and period. More surprisingly, solutions of the seasonal model converge to the coexistence state with annual variation in the interval of bistability ($0.41 < T_s < 0.42$). One could expect that within-year variation, being as large as it is in Figure 6, panel B, would send solutions to the large-amplitude limit cycles instead of keeping them close to the low coexistence point. Determining exactly which initial conditions lead to limit cycles and which to stable



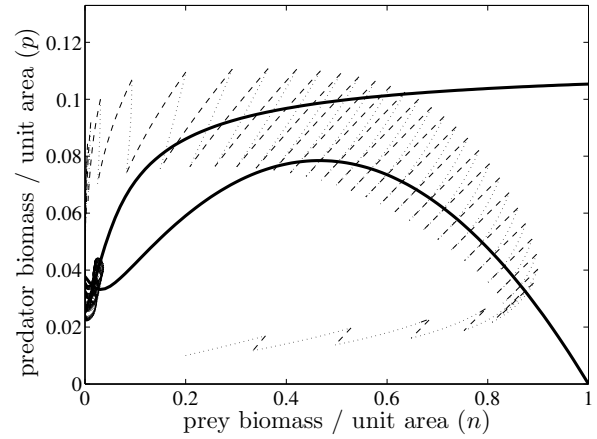
(a) $T_s = 0.58$



(b) $T_s = 0.59$



(c) $T_s = 0.60$



(d) $T_s = 0.62$

Figure 6: Simulation of the seasonal model (3) when summer predation saturates quickly. Panel A: The coexistence state with only annual variation is globally stable when $T_s = 0.4$. Panel B: This state disappears and multi-annual oscillations with large amplitude appear ($T_s = 0.41$). Panel C: The coexistence state at low prey density becomes stable while the large amplitude cycle is still stable ($T_s = 0.42$). Panel D: The low-density coexistence state is globally stable for $T_s = 0.43$. Parameter values are: $\gamma = 0.05, b = 0.05, s = 1, v = 3, m = \mu = 0.4, \alpha = 2, \beta = 0.1$.

coexistence for the seasonal model is beyond the scope of this work.

There are a number of similarities and differences between this and the previous scenario. We still observe the collapse of the high-density coexistence state via a saddle-node bifurcation. This time, however, the alternative steady state is unstable and the system is forced onto a large-amplitude limit cycle. The low prey density state becomes stable as it reaches such low values that the negative feedback generated by the type III functional response is no longer strong enough to drive cyclic behaviour. The large-amplitude cycle still persists in this range, but the maximum of this cycle declines rapidly with increasing summer length, and the cycle disappears when the long summer provides abundant alternative resources for the predator.

Discussion

Many ecosystems experience strong seasonal variation in their environments, particularly at high altitudes or latitudes, and key behaviours of individuals in these ecosystems may change fundamentally with environmental conditions. As individual behaviour, in turn, determines population-level patterns, seasonal variation has the potential to influence the stability of populations. While several studies relate seasonality to disease dynamics (Keeling and Rohani, 2008), there is currently no theory in place for how seasonal variation influences predator-prey systems. To understand how geographic variation and(or) global change affect(s) these ecosystem dynamics, we need to explicitly include seasonality into models. While previous authors have explored predator-prey models with temporally varying strength of predation (Gragnani and Rinaldi, 1995; Rinaldi et al., 1993) or of reproduction and mortality (Hanski and Korpimäki, 1995), our model is the first to vary the qualitative characteristics of a species interaction between seasons. Our model is based on the observations of snowshoe hare and owl functional relationships observed in the boreal forest (Rohner et al., 2001). Their figures 15.6 and 15.9 clearly show the switch from specialist (concave) predation in the winter to generalist (sigmoid) in the summer. The parameter values for our study are chosen from the literature on snowshoe hare and great horned owl. This work thus sheds light on the possible dynamics this system could exhibit with the advance of global change. Our results however, are general and apply to any predator-prey system in which predation behaviour, as measured by the functional response, changes seasonally between that of a generalist and that of a specialist.

We formulated our results in terms of changes in season length. First, we found that changes in season length can affect the strength of the negative feedback cycle and thereby stabilise or destabilise a coexistence state. Second, we found dynamically complex behaviour if the generalist predator has sufficient alternative prey in the summer season. The 'prey extinction' scenario illustrates that internal dynamics could lead to coexisting

stable states (bistability) and eventual prey extinction as a result of increasing summer length. In predator-prey systems, the study of coexisting stable states has received less attention than population cycles. Bistability can arise from a non-monotone functional response (Freedman and Wolkowicz, 1986), from generalist predators (Steele and Henderson, 1992), or from stage-structure (Guill, 2009). Extinction of prey is rare in predator-prey models, but can arise through apparent competition between two prey species (Holt, 1977), even when one prey is held constant (Magal et al., 2008). While we are not explicitly modeling a second prey, we can interpret this bistability and eventual extinction of our focal prey in terms of apparent competition, but with a seasonal dimension. Increasing summer season length can benefit both populations, but the predator, whose alternative food sources are assumed constant throughout the summer, benefits more and drives the focal prey to extinction in the winter, when relying on that prey exclusively. If the predator were a generalist (modeled with a type III functional response) year round, we would not observe extinction (Erbach et al., 2013).

Our results depend on the seasonal switch of the functional response from a sigmoid (Holling type III) to a concave (Holling type II) shape. While the type II response for specialist predators is based on mechanistic theory, the type III response for generalist predation is a phenomenological way to capture ‘prey switching’ (Murdoch, 1969). A mechanistically grounded approach would employ a multi-species functional response (MSFR) (McLellan et al., 2010) for two prey species and hold the density of the second prey constant. This approach is also appealing since statistical tests often fail to detect differences between type II and type III responses from small data sets (Marshall and Boutin, 1999). We investigated the dynamics that result in our seasonal model with the MSFR presented by McLellan et al. (2010) (see their equation (2)). We held the alternative prey density constant during the summer season and set it equal to zero during the winter season. We found that this model can produce qualitatively similar results to those presented in ‘Predator with insufficient alternative resources’ and ‘Scenario 1: Extinction of the Prey’ but not the dynamics that we found in ‘Scenario 2: Large limit cycles’. We conclude that the latter dynamics are only possible if the predator shows some switching behaviour, which the type III response emulates but the approach by McLellan et al. (2010) does not. van Leeuwen et al. (2007) included prey-switching in a mechanistic derivation of a MSFR and found that, for constant alternative prey, a sigmoidal shape emerged. Abrams (1990) had argued that the parameters in the type II response should be density-dependent to model adaptive behaviour in the presence of multiple prey. With appropriately chosen density-dependent rates, a sigmoidal shape can emerge. A detailed study of our system in this general setting remains a future challenge, but we conjecture that our results depend only on the qualitative shape (concave vs. sigmoid) and not on details.

The ‘large limit cycles’ scenario exhibits another case of coexisting stable ‘states’: a stable steady state and a stable limit cycle. Analytically detecting parameter ranges for which such scenarios exist is very difficult (Freed-

man and Wolkowicz, 1986). We suspect that some of the models that show bistability (e.g. Spencer and Collie (1995)) could also exhibit large limit cycles that the authors did not detect, but see Erbach et al. (2013). As a result of this bistable structure, we might observe different dynamic behaviour of the same predator-prey system in functionally identical but geographically different locations, due to initial conditions or one-time disturbances. Previous authors used gradual changes in the amount of generalist predation to understand the geographic variation in the amplitude of vole cycles in Fennoscandia (Turchin and Hanski, 1997). Our seasonal model provides an alternative explanation. In addition, we find that including seasonality can lead to hysteresis if there is a gradual increase in summer season length (due to, for example, global warming), followed by a gradual decrease during temporary cooling periods. Consider Figure 5 when $T_s \approx 0.41$ and assume that the system exhibits large limit cycle oscillations. As summers become longer ($T_s > 0.42$), the limit cycle disappears and gives way to a stable steady state at low population levels. If summers gradually become shorter again, population densities would not resume cycling until $T_s < 0.41$. These changes in T_s translate to changes on the order of a few days in dimensional terms. Changes of this magnitude are consistent with recent and predicted climates in the boreal forest (Allen et al., 2013; Duguay et al., 2006). While an increase in season length of just a few days seems small, the dramatic switch from cyclic to noncyclic dynamics can occur if the system is near a bifurcation point. For ecosystems that rely on keystone species like the snowshoe hare, the difference between oscillatory and steady-state hare dynamics can be profound, especially when steady-state levels are so much lower than the cyclic maxima.

Model complexity

It is clear from these examples that the additional complexity of the seasonal model is necessary to uncover and understand potential system dynamics. Likewise, seasonality is crucial in related predation models (Hanski and Korpimäki, 1995; Taylor et al., 2013; Turchin and Hanski, 1997), in a competition model (Hsu and Zhao, 2012) and in epidemic models (Altizer et al., 2006; Bacaër, 2012). Increased model complexity comes at a price: more data are required for parameter estimation; model analysis is more complicated. We have demonstrated, however, that the analysis can be manageable using techniques such as averaging (see Hsu and Zhao (2012) and discussion below), and that the profound effects of seasonality make it an important consideration in model design. Ideally, data would be gathered in all relevant seasons and used to validate a model. When this is impossible, one should carefully think about how species behaviour might change between seasons. Since data are often collected in a particular season, this very seasonality could be preserved in model design. While the traditional modelling approach assumes that application of the data to all seasons is reasonable, our work indicates that it is worth writing a multi-season model in which the data is applied to the correct season. Then, functional forms and

parameter values for other seasons can be motivated by the single-season data, but not tied to it. In our case, the seasonally driven model, based on data that show the difference between the specialist and generalist functional response (Figure 15.6 in Rohner et al. (2001)) reveals dynamic behaviour that a simplified model, based on summer and winter pooled data (Figure 15.9 in Rohner et al. (2001)) could not possibly contain. We conclude that when data is only available from one season, one needs to carefully consider the possibility of seasonal behaviour change before applying the data to a non-seasonal model.

Model simplification

If seasonal data are available, then how does one analyse the more complicated model structure that results? Explicit numerical simulation is possible but limited; bifurcation analysis is useful but tedious (Gagnani and Rinaldi, 1995; Rinaldi et al., 1993; Taylor et al., 2013). We demonstrated that model simplification via averaging based on a separation of time scales (Guggenheimer and Holmes, 1983) is extremely helpful. From equations (4), we see that rather than pooling the annual data for a single functional response, a better way is to use a linear combination between the functional responses for each season. When intrinsic dynamics are much faster than the environmental forcing, successional-state dynamics can be used to simplify model structure (Klausmeier, 2010). In either case, we advocate that modellers begin by formulating an explicitly seasonal model, and then let the data (e.g. different temporal scales) guide the mathematical approach for model simplification.

Implications for global change scenarios

Ecosystems at high latitudes and altitudes are particularly exposed to the effects of global change. One typically asks whether a species can move fast enough to keep up with the range shift of its optimal habitat (Berestycki et al., 2009; Leroux et al., 2013; Potapov and Lewis, 2004; Zhou and Kot, 2011). We focussed on the local dynamics without movement. We found that when predation varies seasonally, an increase in summer season length can lead to extinction of the prey. It can also generate large limit cycles where minimum densities of prey and predator can be very small, so that stochastic extinction is more likely. Hence, global change endangers populations not only through habitat shift but also through interaction dynamics. A different but related line of research considers the explicit temperature dependence of intraspecific interactions and the effects of mean temperature change on population dynamics (Amarasekare and Coutinho, 2014). Combining our seasonal approach with more detailed data on temperature-dependent processes would allow us to explore not only the effects of mean temperature increases but also the effects of increased variability, an important characteristic of global change (Allen et al., 2013; Easterling et al., 2000; Schär et al., 2004).

In our simple model, only the predation behaviour changes seasonally, but other changes are conceivable and should be included in future models. For example, longer growing seasons can lead to more severe droughts and decreasing resource productivity (Appenzeller, 2015). Timing of reproduction, particularly for species with a single litter per year, could also become important. Another crucial question is how stochastically varying summer lengths affect the somewhat narrow range for T_s where bistability arises. Season length can vary by about 8% (Suni et al., 2003), whereas the range of bistability with the large limit cycle is about 2.5% (Figure 5). We simulated the system by randomly choosing summer length uniformly within $\pm 7\%$ of a mean of $T_s = 0.415$ (Online Appendix B). These simulations show effects of both behaviours: stable coexistence and large limit cycles. Realisations of the stochastic model remain near these deterministic states for some time (depending on stochastic effects and initial conditions) but can also switch between these states at random intervals (Figure B.1, Online Appendix B). When the variation in T_s is small, switching is infrequent; when it is large, realisations spend very little time near the coexistence state and typically show large oscillations.

We focused on a shift in functional response due to seasonally-varying availability of alternative prey. Other drivers for behavioural changes include snow cover, human activities or disturbances that can facilitate or limit predator access to prey (Courbin et al., 2014; McKenzie et al., 2012; Ruediger et al., 2000). Our results demonstrate that such changes can lead to structural changes in predator-prey dynamics that may be difficult to predict. Bistable dynamics are especially challenging for ecosystem management since early warning signs may not exist (Boerlijst et al., 2013). However, few datasets actually measure critical behaviours like the functional response as a seasonally varying quantity. We therefore argue that there is a need for further study of seasonal effects, both empirically and theoretically. From an empirical perspective, we call for data collection in multiple seasons or, at a minimum, the collection of as much information as possible about season-specific behaviours. Theoreticians can then build seasonal models that allow for a thorough investigation of the effect of changing season length, and the identification of patterns that can be tested empirically.

Acknowledgements

FL and RT gratefully acknowledge funding through the Discovery grant program of the National Science and Engineering Research Council of Canada. Some of this work was conceived when both authors visited the Mathematical Biosciences Institute in Columbus, Ohio. We also thank Christina Cobbold for enthusiastic support and inspiring discussions. The authors would also like to thank the anonymous reviewers and editors for many helpful comments that have significantly improved the paper.

Online Appendix A Analytic persistence conditions

In this appendix, we provide some of the explicit calculations that can be carried out to determine persistence conditions of predator and prey in the system as a function of summer season length in a few scenarios.

To start, we note that the prey can persist in the absence of the predator for any positive summer season length since it grows in the summer and – in the absence of a predator – remains constant in the winter. We focus on persistence conditions for the predator, but return to the prey at the end. Throughout this appendix, we use the dimensional versions of the equations, i.e. equations (1) for summer and equations (2) for winter.

Insufficient summer resources

When the maximum predator growth rate from alternative resources is smaller than summer mortality, i.e. $s < m$, then the predator cannot persist in the system without the focal prey. The necessary and sufficient conditions for predator persistence in this case can be determined explicitly by invasion analysis.

The standard, non-seasonal, generalist predator model, given in equations (1), has the prey-only steady state $(K, 0)$. The predator can invade this state and persist in the system if the state is unstable. Linearizing the predator equation at this state gives the instability condition

$$\frac{\gamma a K^2}{b^2 + K^2} + s > m. \quad (\text{A.1})$$

The seasonal model with equations (1) and (2) still has the constant solution $(K, 0)$ as the prey-only state since, in the absence of the predator, the prey remains constant in the winter. The linearized growth rates of the predator during summer and winter, respectively, are

$$\rho_1 = \frac{\gamma a K^2}{b^2 + K^2} + s - m \quad \text{and} \quad \rho_2 = \frac{\gamma \alpha K}{\beta + K} - \mu. \quad (\text{A.2})$$

The predator can persist in the system if the combined growth effects from the two seasons (the Liapunov exponent) is greater than unity. Since the predator grows (approximately) linearly with rate ρ_1 for time T_s and with rate ρ_2 for time $(1 - T_s)$, the combined annual growth rate is given by

$$R^* = e^{\rho_1 T_s} e^{\rho_2 (1 - T_s)} = e^{\rho_1 T_s + \rho_2 (1 - T_s)}. \quad (\text{A.3})$$

The predator can persist exactly if $R^* > 1$ or, equivalently, $\rho_1 T_s + \rho_2 (1 - T_s) > 0$.

Sufficient summer resources

When the maximum predator growth rate from alternative resources is larger than summer mortality, i.e. $s > m$, then the predator can persist in the system without the focal prey, provided the summer season is long enough. Linearizing the predator equation at the trivial state $(0, 0)$, one finds the summer growth rate as $s - m > 0$ and the winter death rate as μ , so that the combined annual growth rate is

$$R^{**} = e^{(s-m)T_s - \mu(1-T_s)}. \quad (\text{A.4})$$

Accordingly, the predator can persist in the absence of the focal prey if $R^{**} > 1$ or, equivalently, $T_s > \mu / (\mu + s - m)$. If this condition is satisfied, the predator density on its own will approach a solution with only annual variation (also called an ‘impulsive periodic orbit’), where it decays exponentially in the winter and grows logistically in the summer. We denote this state by $P^*(t)$: It is a periodic function with period 1.

Prey persistence

Finally, we can ask whether the prey can grow from low density if the predator is established in the scenario of sufficient summer resources. Linearizing the prey equation at the state $(0, P^*(t))$ gives the prey growth rate r in the summer and $-\alpha P^*(t)$ in the winter. The combined annual growth rate is then

$$R_* = \exp \left(rT_s - \int_{T_s}^1 \alpha P^*(t) dt \right). \quad (\text{A.5})$$

Since the predator density $P^*(t)$ is exponentially decreasing during the winter, we can evaluate the integral and find that the prey can grow from low density if

$$rT_s - \frac{\alpha P^*(T_s)}{\mu} \left(1 - e^{-\mu(1-T_s)} \right) > 0. \quad (\text{A.6})$$

In other words, if the predator density at the end of the summer/beginning of the winter, $P^*(T_s)$ is small enough, then the prey can invade the system and persist. Unfortunately, an explicit expression for $P^*(T_s)$ is unavailable, but we can find an implicit expression.

From the winter dynamics in the absence of the prey, we find that $P^*(1) = e^{-\mu(1-T_s)} P^*(T_s)$. Since $P^*(1)$ is the initial predator density at the beginning of the next summer, we need to solve the equation

$$\frac{dP}{dt} = \frac{sP}{1 + vP} - mP \quad (\text{A.7})$$

with initial condition $P_0 = P^*(1)$ from time $t = 0$ until $t = T_s$ to obtain an implicit expression for $P^*(T_s)$. The differential equation is separable, and after tedious calculations, we find

$$\frac{P^*(T_s)}{(s - m - mvP^*(T_s))^{s/m}} - \frac{P^*(T_s)e^{-\mu(1-T_s)}}{(s - m - mvP^*(T_s)e^{-\mu(1-T_s)})^{s/m}} = e^{(s-m)T_s} - 1 \quad (\text{A.8})$$

as the defining equation for $P^*(T_s)$.

Online Appendix B Stochastic variation in summer season length

In this appendix, we report on some simulation results, in which the summer season length varied stochastically. In ‘Scenario 2: Large limit cycles’, we observed bistability between a steady state and a limit cycle for a relatively narrow range of T_s . The inter-annual variability of growing season length may be larger than that range, for example, Suni et al. (2003) observed a minimum and maximum growing season length of 182 and 214 days, respectively in a 5-year period, which corresponds to about 8% variation. By comparison, the bistability range of T_s in Figure 5, panel B, represents only about 2.5% variation in time. (Please note, however, that this value is scaled, and the range of T_s in original parameters depends on the value of r .) Would one expect to see bistability at all if summer season length varied stochastically?

To answer this question, we simulated the model with a mean summer season length of $T_s = 0.415$ in the region of bistability in Figure 5, panel B. The actual season length was chosen randomly from a uniform distribution, centered at $T_s = 0.415$ and a width of $\pm 7\%$. Only season length was varied stochastically, within each season the deterministic dynamics were simulated.

From the representative results in Figure B.1 we observe that the bistable nature of the deterministic system is still visible in the stochastic simulations. Some solutions remain near the deterministic steady state for the simulated 500 years, others remain near the deterministic limit cycle for the same time. Stochasticity allows some realizations of the process to switch from near the limit cycle to near the coexistence state and vice versa. For smaller ranges of stochastic variation, this switching behaviour was observed less frequently; for larger range, realizations of the process seemed to spend increasingly more time near the deterministic limit cycle (plots not shown). The switching behaviour of stochastic realizations of a deterministic system with alternative stable states has been explored quite recently (Sharma et al., 2015). A detailed study of the effect of stochasticity on the bistable situation with limit cycle is still open.

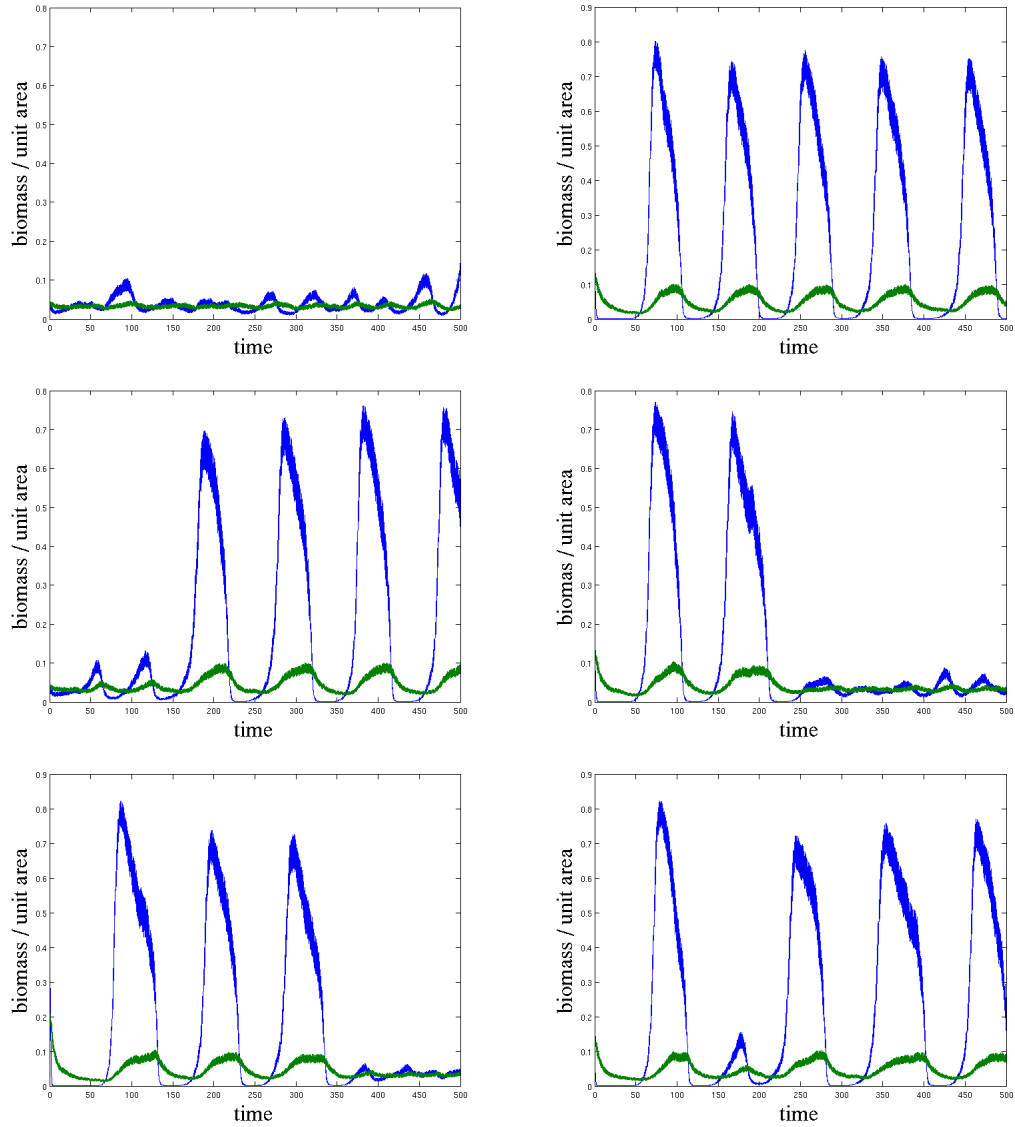


Figure B.1: Representative realizations of the stochastic process that results from choosing summer season length in model (3) a stochastic variable. We chose T_s from a uniform distribution on $0.415 \pm 7\%$. The top left panel shows that solutions can stay near the deterministic coexistence state for a long time; the top right panel shows that they can stay near the deterministic limit cycle for a long time. The other panels show that solutions can switch between these two states in either direction and after long or short times. Initial conditions were chosen such that (i) deterministic solutions converged to the coexistence state (left: top and middle), (ii) deterministic solutions converged to the limit cycles (right: top and middle), and (iii) randomly (bottom plots).

References

- Abrams, P. 1990. The effects of adaptive behavior on the type-2 functional response. *Ecology* 71:877–885.
- Allen, M., O. Boucher, D. Chambers, J. Christensen, P. Ciais, P. Clark, M. Collins, J. Comiso, V. de Menezes, R. Feely, T. Fichfet, A. Fiore, G. Flato, J. Fuglestedt, G. Hegerl, P. Hezel, G. Johnson, G. Kaser, V. Kattsov, J. Kennedy, A. Tank, C. L. Qu  r  , G. Myhre, T. Osborn, A. Payne, J. Perlwitz, S. Power, M. Prather, S. Rintoul, J. Rogelj, M. Rusticucci, M. Schulz, J. Sedl  cek, P. Stott, R. Sutton, P. Thorne, and D. Wuebbles. 2013. *Climate change 2013: The physical science basis*. Tech. Rep. AR5, Intergovernmental Panel on Climate Change.
- Altizer, S., A. Dobson, P. Hosseini, P. Hudson, M. Pascual, and P. Rohani. 2006. Seasonality and the dynamics of infectious diseases. *Ecology Letters* 9:467–484.
- Amarasekare, P., and R. Coutinho. 2014. Effects of temperature on intraspecific competition in ectotherms. *American Naturalist* 184:E50–E65.
- Appenzeller, T. 2015. The new north. *Science* 349:806–809.
- Baca  r, N. 2012. The model of Kermack and McKendrick for the plague epidemic in Bombay and the type reproduction number with seasonality. *Journal of Mathematical Biology* 64:403–422.
- Berestycki, H., O. Diekmann, C. Nagelkerke, and P. Zegeling. 2009. Can a species keep pace with a shifting climate? *Bulletin of Mathematical Biology* 71:399–429.
- Berryman, A. 1989. The conceptual foundations of ecological dynamics. *Bulletin of the Ecological Society of America* 70:230–236.
- Bj  rnstad, O., C. Robinet, and A. Liebhold. 2010. Geographic variation in North American gypsy moth cycles: subharmonics, generalist predators, and spatial coupling. *Ecology* 91:106–118.
- Boerlijst, M., T. Oudman, and A. de Roos. 2013. Catastrophic collapse can occur without early warning: Examples of silent catastrophes in structured ecological models. *PLoS ONE* 8:e62033.
- Courbin, N., D. Fortin, C. Dussault, and R. Courtois. 2014. Logging-induced changes in habitat network connectivity shape behavioural interactions in the wolf-caribou-moose system. *Ecological Monographs* 84:265–285.
- Duguay, C., T. Prowse, B. Bonsal, R. Brown, M. Lacroix, and P. M  nard. 2006. Recent trends in Canadian lake ice cover. *Hydrological Processes* 20:781–801.

- Easterling, D., G. Meehl, C. Parmesan, S. Changnon, T. Karl, and L. Mearns. 2000. Climate extremes: Observations, modeling, and impacts. *Science* 289:2068–2074.
- Erbach, A., F. Lutscher, and G. Seo. 2013. Bistability and limit cycles in generalist predator-prey dynamics. *Ecological Complexity* 14:48–55.
- Freedman, H., and G. Wolkowicz. 1986. Predator-prey systems with group defence: the paradox of enrichment revisited. *Bulletin of Mathematical Biology* 48:493–508.
- Gagnani, A., and S. Rinaldi. 1995. A universal bifurcation diagram for seasonally perturbed predator-prey models. *Bulletin of Mathematical Biology* 57.
- Guckenheimer, J., and P. Holmes. 1983. *Nonlinear Oscillations, Dynamical Systems and Bifurcation of Vector Fields*. Springer-Verlag.
- Guill, C. 2009. Alternative dynamical states in stage-structured consumer populations. *Theoretical Population Biology* 76:168–178.
- Hanski, I., and E. Korpimäki. 1995. Microtine rodent dynamics in the northern Europe: parameterized models for the predator-prey interaction. *Ecology* 76:840–850.
- Hodges, K., C. Krebs, D. Hik, C. Stefan, E. Gillis, and C. Doyle. 2001. Snowshoe hare demography. Chap. 8, pages 141–178 in C. Krebs, S. Boutin, and R. Boonstra, eds. *Ecosystem Dynamics of the Boreal Forest: The Kluane Project*. Oxford University Press, Oxford; New York.
- Holling, C. 1959. The components of predation as revealed by a study of small-mammal predation of the European pine sawfly. *Canadian Entomologist* 91:293–320.
- Holt, R. 1977. Predation, apparent competition, and the structure of prey communities. *Theoretical Population Biology* 12:197–229.
- Houston, C., and C. Francis. 1995. Survival of Great Horned Owls in relation to the snowshoe hare cycle. *Auk* 112:44–59.
- Houston, C., D. Smith, and C. Rohner. 1998. Great horned owl (*Bubo virginianus*). In A. Poole and F. Gill, eds., *The Birds of North America Online*. The Birds of North America Online, Ithaca, NY. Revision: May 16, 2014 by C. Artuso and C.S. Houston.

- Hsu, S.-B., and X.-Q. Zhao. 2012. A Lotka-Volterra competition model with seasonal succession. *Journal of Mathematical Biology* 64:109–130.
- IPCC Working Group I. 2007. Projections of future changes in climate. IPCC Publications and Data. [Http://www.ipcc.ch/publications_and_data/ar4/wg1/en/spmsspmpm-projections-of.html](http://www.ipcc.ch/publications_and_data/ar4/wg1/en/spmsspmpm-projections-of.html).
- Keeling, M., and P. Rohani. 2008. *Modelling Infectious Diseases in Humans and Animals*. Princeton University Press, Princeton, NJ.
- King, A., and W. Schaffer. 2001. The geometry of a population cycle: A mechanistic model of snowshoe hare demography. *Ecology* 82:814–830.
- Klausmeier, C. 2010. Successional state dynamics: A novel approach to modeling nonequilibrium foodweb dynamics. *Journal of Theoretical Biology* 262:584–595.
- Leroux, S., M. Larrivé, V. Boucher-Lalonde, A. Hurford, J. Zuloga, J. Kerr, and F. Lutscher. 2013. Mechanistic models for the spatial spread of species under climate change. *Ecological Applications* 23:815–828.
- Ludwig, D., D. Jones, and C. Holling. 1978. Qualitative analysis of insect outbreak systems: the spruce budworm and the forest. *Journal of Animal Ecology* 47:315–332.
- Magal, C., C. Cosner, and S. Ruan. 2008. Control of invasive hosts by generalist parasitoids. *Mathematical Medicine and Biology* 25:1–20.
- Marshall, J., and S. Boutin. 1999. Power analysis of wolf-moose functional responses. *Journal of Wildlife Management* 63:396–402.
- Maynard Smith, J. 1974. *Models in Ecology*. Cambridge University Press, Cambridge, United Kingdom.
- McKenzie, H., E. Merrill, R. Spiteri, and M. Lewis. 2012. How linear features alter predator movement and the functional response. *Interface Focus* pages 205–216.
- McLellan, B., R. Serrouya, H. Wittmer, and S. Boutin. 2010. Predator-mediated Allee effects in multi-prey systems. *ecology* 91:286-2. *Ecology* 91:286–292.
- Miller, D., J. Grand, T. Fondell, and M. Anthony. 2006. Predator functional response and prey survival: direct and indirect interactions affecting a marked prey population. *Journal of Animal Ecology* 75:101–110.

- Molnàr, P., A. Derocher, G. Thiemann, and M. Lewis. 2010. Predicting survival, reproduction and abundance of polar bears under climate change. *Biological Conservation* 143:1612–1622.
- Morozov, A., and S. Petrovskii. 2009. Excitable population dynamics, biological control failure, and spatiotemporal pattern formation in a model ecosystem. *Bulletin of Mathematical Biology* 71:863–887.
- Murdoch, W. 1969. Switching in generalist predators: experiments on prey specificity and stability of prey populations. *Ecological Monographs* 39:335–354.
- Patterson, B., L. Benjamin, and F. Messier. 1998. Prey switching and feeding habits of eastern coyotes in relation to snowshoe hare and white-tailed deer densities. *Canadian Journal of Zoology* 76:1885–1897.
- Potapov, A., and M. Lewis. 2004. Climate and competition: The effect of moving range boundaries on habitat invasibility. *Bulletin of Mathematical Biology* 66:975–1008.
- Rinaldi, S., S. Muratori, and Y. Kuznetsov. 1993. Multiple attractors, catastrophes, and chaos in seasonally perturbed predator-prey communities. *Bulletin of Mathematical Biology* 55:15–35.
- Rohner, C., F. Doyle, and J. Smith. 2001. Great horned owls. Chap. 15, pages 339–376 in C. Krebs, S. Boutin, and R. Boonstra, eds. *Ecosystem Dynamics of the Boreal Forest: The Kluane Project*. Oxford University Press, Oxford; New York.
- Ruediger, B., J. Claar, S. Mighton, B. Naney, T. Rinaldi, F. Wahl, N. Warren, D. Wenger, A. Williamson, L. Lewis, B. Holt, G. Patton, J. Trick, A. Vandehey, and S. Gniadek. 2000. Canada Lynx conservation assessment and strategy. Tech. Rep. 1-132, United States Fish and Wildlife Service.
- Ruggerio, L., K. Aubry, S. Buskirk, G. Koehler, C. Krebs, K. McKelvey, and J. Squires. 2000. *Ecology and Conservation of Lynx in the United States*. University Press of Colorado, Niwot, Colorado.
- Schär, C., P. L. Vidale, D. Lüthi, and C. Frei. 2004. The role of increasing temperature variability in European summer heatwaves. *Nature* 427:3926–3928.
- Sharma, Y., K. Abbott, P. Dutta, and A. Gupta. 2015. Stochasticity and bistability in insect outbreak dynamics. *Theoretical Ecology* 8:163–174.
- Smith, D., and J. Murphy. 1979. Breeding responses of raptors to jackrabbit density in the eastern Great Basin desert of Utah. *Raptor Research* 13:1–14.

- Spencer, P., and J. Collie. 1995. A simple predator-prey model of exploited marine fish populations incorporating alternative prey. *ICES Journal of Marine Science* 53:615–628.
- Steele, J., and E. Henderson. 1992. The role of predation in plankton models. *Journal of Plankton Research* 14:157–172.
- Strohm, S., and R. Tyson. 2009. The effect of habitat fragmentation on cyclic population dynamics: A numerical study. *Bulletin of Mathematical Biology* 71:1323–1348.
- Suni, T., F. Berninger, T. Markkanen, P. Keronen, U. Rannik, and T. Vesala. 2003. Interannual variability and timing of growing-season CO₂ exchange in a boreal forest. *Journal of Geophysical Research* 108:4265.
- Taylor, R., J. Sherratt, and A. White. 2013. Seasonal forcing and multi-year cycles in interacting populations: lessons from a predator-prey model. *Journal of Mathematical Biology* 67:1741–1764.
- Turchin, P., and I. Hanski. 1997. An empirically based model for latitudinal gradient in vole population dynamics. *American Naturalist* 149:842–874.
- Tyson, R. 2016. Matlab code for: Seasonally varying predation behaviour and climate shifts are predicted to affect predator-prey cycles. *The American Naturalist*, Dryad Digital Repository, <http://doi:10.5061/dryad.f2mk6>.
- Tyson, R., S. Haines, and K. Hodges. 2010. Modelling the Canada lynx and snowshoe hare population cycle: The role of specialist predators. *Theoretical Ecology* 3:97–111.
- van Leeuwen, E., V. Jansen, and P. Bright. 2007. How population dynamics shape the functional response in a one-predator-two-prey system. *Ecology* 88:1571–1581.
- Zhou, Y., and M. Kot. 2011. Discrete-time growth-dispersal models with shifting species ranges. *Theoretical Ecology* 4:13–25.

Param.	Description	Units	Range	Source
r	prey summer growth rate	/year	1.5-2.0	(a), (d)
K	prey summer carrying capacity	hares/ha	4.0-8.0 (12)	(a), (c)
α	specialist saturation killing rate	hares/owl/year	50-150 (250)	(b)
β	specialist half saturation	hares/ha	0.05-0.25	(b)
γ	conversion efficiency	owls/hare	0.007-0.012	(f)
m/μ	summer/winter predator death rate	/year	0.14-0.6	(g)
a	generalist saturation killing rate	hares/owl/year	$110 \pm 15\%$	(e)
b	generalist half-saturation	hares/ha	$1 \pm 15\%$	(e)
s	generalist predator max. growth rate	/year	1.4	(f)
ν	generalist predator density-dependence	/owl	unknown	

Table B.1: Model parameters, their units and numerical values (dimensional) with references. Numbers in parenthesis are outliers reported in isolated studies. Many of the parameter values were obtained from previous modelling work (Tyson et al., 2010). The values reported there were obtained from the following sources: (a) Hodges et al. (2001), (b) Rohner et al. (2001), (c) Ruggerio et al. (2000), and (d) King and Schaffer (2001). Source (e) indicates parameters obtained through a least-squares fitting of the functional forms to the data in Figure 15.9 of Rohner et al. (2001). Since this fitting yielded only a single value for each parameter, we assumed that there was $\pm 15\%$ variation possible. This is considerably less than the variation exhibited in the other parameter values except r . Source (f) indicates parameters derived using demographic parameters retrieved from Houston et al. (1998) and Smith and Murphy (1979). Source (g) indicates parameters derived using demographic parameters retrieved from Houston et al. (1998) and Houston and Francis (1995). Note that the two saturation killing rates, α and a , are the product of the encounter rate and the probability of making the kill at each encounter.

List of Figures

- Two typical long-term scenarios in the two-season model (3): Annual variation (panels A and C) and multi-annual cycles (panels B and D). In the phase-plane plots (panels A and B), arrows indicate the direction of solutions during the summer (solid lines) and winter (dashed lines). Corresponding time series plots (panels C and D) show prey density of the annual model (solid lines) and the averaged model (dash-dotted lines). Asterisks indicate annual averages of the seasonal model. . . . 7
- Solution trajectories of the seasonal model (3) in the phase plane for three different values of T_s . Solution trajectories in Panels A and C include transient and steady state behaviour; the solution trajectory in Panel B shows only the long-term behaviour. The steady-state behaviour in each case is: (A) Annual variation for $T_s = 0.55$. (B) Multi-annual cycles for $T_s = 0.75$. (C) Annual variation for $T_s = 0.9$. Solid lines correspond to nullclines of the averaged model (4). Parameters are $b = 0.25$, $\alpha = 2$, $\beta = 0.05$, $s = 0.5$, $m = \mu = 0.6$. and $\gamma = 0.25$ 9

- 3 Panel A: Prey density as a function of summer season length: average of the seasonal model (solid) and averaged model (dashed). Maximal and minimal values are plotted after transients have disappeared. Panel B: Stability as a function of T_s and α for small (dashed) and large (solid) values of b (solid lines: $b = 0.5$, dashed lines: $b = 0.23$). For each pair of lines (solid or dashed) there is a thin line and a thick line. Below the thin line, the predator cannot persist in the system according to (7). Between the thin and thick lines, predator and prey stably coexist. Above the thick lines, the populations cycle. All other parameters are as in Figure 2. 10
- 4 Simulation of the seasonal model (3) when the generalist predator has sufficient alternative resources to survive in the absence of prey. Solution trajectories shown include transient and steady-state behaviour. Panel A: The coexistence state with only annual variation is globally stable when $T_s = 0.58$. Panels B and C: The coexistence state and the prey extinction state are both locally stable when $T_s = 0.59$ and $T_s = 0.6$. In the latter case, the annual averages approach the coexistence state with damped oscillations. Solution trajectories for two different initial conditions are shown. Panel D: The prey extinction state is globally stable when summers are long, $T_s = 0.62$. Parameter values are: $\gamma = 0.07, b = 0.25, s = 1, v = 3, m = \mu = 0.5, \alpha = 2, \beta = 0.08$ 13
- 5 Qualitative behaviour of the seasonal (3) and averaged (4) model as a function of summer season length. Panel A: Prey extinction scenario. Panel B: Large limit cycle scenario. Thin solid lines indicate the prey steady-state value in the averaged model. Thin dashed lines represent the maximum and minimum of an unstable limit cycle. Asterisks correspond to simulation results (maxima and minima after the disappearance of initial transients) of the averaged model (4) with two different initial conditions (one in the basin of attraction of the upper steady state, and one outside of this basin and leading to prey extinction). Open circles indicate the corresponding simulations of the seasonal model (3). SN denotes a saddle-node bifurcation in the averaged model, T a transcritical bifurcation. SH stands for subcritical Hopf bifurcation, HL and SNL indicate a homoclinic loop bifurcation and a saddle-node bifurcation of limit cycles (see explanation in the text). The vertical dash-dot lines only serve to provide visual structure to the reader. In panel B, the homoclinic loop bifurcation occurs just before the saddle-node bifurcation. Parameter values are $\gamma = 0.07, b = 0.25, s = 1, v = 3, m = \mu = 0.5, \alpha = 2$, and $\beta = 0.08$ for panel A and $\gamma = 0.05, b = 0.05, s = 1, v = 3, m = \mu = 0.4, \alpha = 2$, and $\beta = 0.1$ for panel B. 14

6 Simulation of the seasonal model (3) when summer predation saturates quickly. Panel A: The coexistence state with only annual variation is globally stable when $T_s = 0.4$. Panel B: This state disappears and multi-annual oscillations with large amplitude appear ($T_s = 0.41$). Panel C: The coexistence state at low prey density becomes stable while the large amplitude cycle is still stable ($T_s = 0.42$). Panel D: The low-density coexistence state is globally stable for $T_s = 0.43$. Parameter values are: $\gamma = 0.05, b = 0.05, s = 1, v = 3, m = \mu = 0.4, \alpha = 2, \beta = 0.1$ 16

B.1 Representative realizations of the stochastic process that results from choosing summer season length in model (3) a stochastic variable. We chose T_s from a uniform distribution on $0.415 \pm 7\%$. The top left panel shows that solutions can stay near the deterministic coexistence state for a long time; the top right panel shows that they can stay near the deterministic limit cycle for a long time. The other panels show that solutions can switch between these two states in either direction and after long or short times. Initial conditions were chosen such that (i) deterministic solutions converged to the coexistence state (left: top and middle), (ii) deterministic solutions converged to the limit cycles (right: top and middle), and (iii) randomly (bottom plots). 27